# Brain atrophy patterns in anti-IgLON5 disease

- 2 Selina M. Yogeshwar, <sup>1,2</sup> Frederik Bartels, <sup>1,3,4,5</sup> Thomas Grüter, <sup>6,7</sup> Sergio Muñiz-Castrillo, <sup>8,9</sup>
- 3 Géraldine Picard, 8,10 Yvette S. Crijnen, 11 Emilien Bernard, 12 Anna Heidbreder, 13 Anastasia
- 4 Zekeridou, <sup>14,15,16</sup> Marius Ringelstein, <sup>17,18</sup> Andrea Kraft, <sup>19</sup> Stjepana Kovac, <sup>20</sup> Klaus-Peter
- Wandinger,<sup>21</sup> Juna M. de Vries,<sup>11</sup> Agnita J. W. Boon,<sup>11</sup> Sharon Veenbergen,<sup>22</sup> Christian Geis,<sup>23</sup>
- 6 Loana Penner, <sup>24,25</sup> Nico Melzer, <sup>17</sup> Frank Leypoldt, <sup>21,26</sup> Morten Blaabjerg, <sup>27,28</sup> Sean J. Pittock, <sup>15,16</sup>
- 7 Carles Gaig,<sup>29</sup> Lidia Sabater,<sup>30,31,32</sup> Joan Santamaria,<sup>29</sup> Francesc Graus,<sup>29</sup> Josep Dalmau,<sup>29,33,34</sup>
- 8 Harald Prüss,<sup>1,35</sup> Romana Höftberger,<sup>36,37</sup> Bettina Schreiner,<sup>38,39</sup> Andrew McKeon,<sup>14</sup> Jan
- 9 Lewerenz,<sup>24</sup> Sarosh Irani,<sup>40,41,42</sup> Emmanuel Mignot,<sup>43</sup> Maarten J. Titulaer,<sup>11</sup> Ilya Ayzenberg,<sup>6,†</sup>
- Jérôme Honnorat<sup>8,†</sup> and Carsten Finke<sup>1,44,†</sup> for the IgLON5 Imaging Consortium

#### †These authors contributed equally to this work.

12

13

11

1

### **Abstract**

- Anti-IgLON5 disease is an autoimmune encephalitis that presents with a heterogenous clinical
- 15 phenotype, including sleep disorders, movement abnormalities and bulbar involvement. It is
- characterised by autoantibodies against IgLON5, 85% association with *HLA-DQB1\*05:*~ and a
- brainstem-dominant tauopathy. Cellular and murine models report pathogenic effects of the
- autoantibodies, and neurodegenerative factors suggest progressive atrophy as a common sequela.
- 19 However, evidence from *in vivo* patient data and long-term follow up are limited. Further, the
- 20 degree of progression remains elusive.
- 21 In this multi-centre study, clinical and brain MRI data were collected from 127 patients across
- 22 twelve countries to investigate the relationships between clinical presentations and the
- 23 development of distinct brain atrophy patterns. Our data show that most patients develop a
- 24 complex multi-system phenotype as the disease progresses, however, neuromuscular
- 25 manifestations rarely emerge at later disease stages. By comparison to healthy controls, this disease
- 26 presents with severe sub-structure specific atrophy, especially affecting the hypothalamus,
- brainstem, accumbens and basal ganglia which, in age-independent analyses, show significant © The Author(s) 2025. Published by Oxford University Press on behalf of The Guarantors of Brain. This is an Open Access article distributed under the terms of the Creative Commons Attribution License (https://creativecommons.org/licenses/by/4.0/), which permits unrestricted reuse, distribution, and reproduction in any medium, provided the original work is properly cited.

- 1 ventricular enlargement and also suggest progression of brainstem atrophy over the disease course.
- 2 Moreover, the focality of atrophy was functionally linked to specific symptoms, with more severe
- 3 involvement of the basal ganglia in patients with movement disorders, and greater atrophy in the
- 4 hippocampus and thalamus in patients with cognitive impairment.
- 5 Taken together, our results provide evidence of distinct atrophy patterns in anti-IgLON5 disease,
- 6 which closely mirror sites of pathophysiologic processes, including autoantibody binding and tau
- 7 deposition. Our data emphasize the brainstem as the pathophysiological hub of the disease and
- 8 provide normative data for the incorporation of atrophy measurements into routine clinical
- 9 assessments and future treatment studies to monitor disease trajectory and evaluate future
- 10 treatment strategies.

#### 12 Author affiliations:

- 13 1 Department of Neurology and Experimental Neurology, Charité-Universitätsmedizin Berlin,
- 14 Corporate Member of Freie Universität Berlin, Humboldt-Universität Berlin, Berlin, 10117,
- 15 Germany
- 16 2 Einstein Center for Neurosciences Berlin, Charité- Universitätsmedizin Berlin, Berlin, 10117,
- 17 Germany
- 18 3 Institute for Immunity, Transplantation, and Infection, Stanford University School of Medicine,
- 19 Stanford, CA 94305, USA
- 4 Berlin Institute of Health at Charité Universitätsmedizin Berlin, Berlin, 10178, Germany
- 5 Berlin School of Mind and Brain, Humboldt-Universität zu Berlin, Berlin, 10117, Germany
- 22 6 Department of Neurology, St. Josef Hospital, Ruhr University Bochum, Bochum, 44791,
- 23 Germany
- 7 Department of Neurology, Evangelic Hospital Lippstadt, Lippstadt, 59555, Germany
- 25 8 French Reference Centre on Paraneoplastic Neurological Syndromes and Autoimmune
- 26 Encephalitis, Hospices Civils de Lyon, Lyon, 69677, France
- 9 Department of Neurology, Hospital Universitario 12 de Octubre, Madrid, 28041, Spain

- 1 10 MeLiS UCBL-CNRS UMR 5284 INSERM U1314, Université Claude Bernard Lyon 1,
- 2 Lyon, 69372, France
- 3 11 Department of Neurology, Erasmus University Medical Center, Rotterdam, 3015GD, The
- 4 Netherlands
- 5 12 Lyon ALS Reference Center, Hôpital Neurologique Pierre Wertheimer, Hospices Civils de
- 6 Lyon, Université de Lyon, Bron, 69677, France
- 7 13 Department of Neurology, Johannes Kepler University Linz, Linz, 4020, Austria
- 8 14 Department of Laboratory Medicine and Pathology, Mayo Clinic, Rochester, MN 55905, USA
- 9 15 Department of Neurology, Mayo Clinic, Rochester, MN 55905, USA
- 10 16 Center for Multiple Sclerosis and Autoimmune Neurology, Mayo Clinic, Rochester, MN
- 11 55905, USA
- 12 17 Department of Neurology, Medical Faculty and University Hospital, Heinrich-Heine-
- 13 University Düsseldorf, 40225 Düsseldorf, Germany
- 14 18 Department of Neurology, Center for Neurology and Neuropsychiatry, LVR-Klinikum,
- 15 Heinrich-Heine-University Düsseldorf, Düsseldorf, 40629, Germany
- 16 19 Department of Neurology, Martha-Maria Hospital Halle, Halle, 06120, Germany
- 17 20 Department of Neurology with Institute of Translational Neurology, University of Münster,
- 18 Münster, 48149, Germany
- 19 21 Institute of Clinical Chemistry, University Hospital Schleswig-Holstein, Kiel, 24105, Germany
- 20 22 Laboratory of Medical Immunology, Department of Immunology, Erasmus University Medical
- 21 Center, University Medical Center, Rotterdam, 3015GD, The Netherlands
- 22 23 Section Translational Neuroimmunology, Jena University Hospital, Jena, 07747, Germany
- 24 Department of Neurology, University Hospital Ulm, Ulm, 89081, Germany
- 24 25 Department of Pediatrics, University Hospital Schleswig-Holstein, Lübeck, 23562, Germany
- 25 26 Department of Neurology, University Hospital Schleswig-Holstein, Kiel, 24105, Germany
- 26 27 Department of Neurology, Odense University Hospital, Odense, 5000, Denmark

- 1 28 Department of Clinical Research, University of Southern Denmark, Odense, 5230, Denmark
- 2 29 Neurology Service, Hospital Clínic of Barcelona, Biomedical Research Institute (IDIBAPS),
- 3 Barcelona, 08036, Spain
- 4 30 Neuroimmunology Program, Fundació de recerca clínic Barcelona-Institut d'Investigacions
- 5 Biomèdiques August Pi i Sunyer (FCRB-IDIBAPS) Caixa Research Intitute (CRI), Barcelona,
- 6 08036, Spain
- 7 31 Universitat de Barcelona, Barcelona, 08036, Spain
- 8 32 Centro de Investigación Biomédica en Red, Enfermedades raras (CIBERER), Madrid, 28029,
- 9 Spain
- 10 33 IDIBAPS Caixa Research Institute, Barcelona, 08036, Spain
- 11 34 Department of Neurology, University Pennsylvania, PA 19104, USA
- 12 35 German Center for Neurodegenerative Diseases (DZNE) Berlin, Berlin, 10117, Germany
- 13 36 Division of Neuropathology and Neurochemistry, Department of Neurology, Medical
- 14 University of Vienna, Vienna, 1090, Austria
- 15 37 Comprehensive Center for Clinical Neurosciences and Mental Health, Medical University of
- 16 Vienna, Vienna, 1090, Austria
- 17 38 Department of Neurology, University Hospital Zurich, Zurich, 8091, Switzerland
- 18 39 Institute of Experimental Immunology, University of Zurich, Zurich, 8057, Switzerland
- 19 40 Department of Neurology, Mayo Clinic, Jacksonville, FL 32224, USA
- 20 41 Department of Neurosciences, Mayo Clinic, Jacksonville, FL 32224, USA
- 21 42 Oxford Autoimmune Neurology Group, Nuffield Department of Clinical Neurosciences, 9
- 22 University of Oxford, Oxford, OX3 9DU, UK
- 23 43 Stanford Center for Sleep Sciences and Medicine, Stanford University School of Medicine,
- 24 Stanford, CA 94305, USA
- 25 44 Berlin Center for Advanced Neuroimaging, Charité- Universitätsmedizin Berlin, Corporate
- 26 Member of Freie Universität Berlin and Humboldt-Universität zu Berlin, Berlin, 10117, Germany

- 1 Correspondence to: Professor Carsten Finke
- 2 Department of Neurology and Experimental Neurology, Charité-Universitätsmedizin Berlin,
- 3 Corporate Member of Freie Universität Berlin, Humboldt-Universität Berlin, 10117, Berlin,
- 4 Germany
- 5 E-mail: carsten.finke@charite.de
- 6 ORCID ID: 0000-0002-7665-1171

- 8 **Running title**: Atrophy in anti-IgLON5 disease
- 9 **Keywords:** autoimmune encephalitis; IgLON5; MRI; atrophy

10

11

### Introduction

- 12 Anti-IgLON5 disease predominantly affects patients above the age of 60 years, showing a
- 13 heterogeneous clinical presentation<sup>1</sup> involving sleep, bulbar, movement, neuromuscular and
- 14 cognitive manifestations<sup>2,3</sup>. The majority of patients present with a multi-system phenotype<sup>4</sup>.
- 15 Response to immunotherapy varies depending on disease stage, with only half of those treated
- showing an improvement<sup>4,5</sup>. The key autoimmune hallmark of the disease are autoantibodies
- 17 targeting IgLON5 that disrupt cytoskeletal organisation, reduce synaptic protein content,
- 18 contribute to an inflammatory response, and lead to both p-tau accumulation and cell death<sup>6-9</sup>.
- 19 Moreover, the disease is 85% associated with HLA-DOA1\*01:05~DOB1\*05:01, HLA-
- 20  $DQA1*01:01\sim DQB1*05:01$  and  $HLA-DQA1*01:04\sim DQB1*05:03$  haplotypes<sup>10</sup> (denoted as HLA-
- 21 DQB1\*05:~ in the rest of the text). These encode HLA molecules that bind IgLON5-derived
- 22 peptides, evoking elevated CD4<sup>+</sup> T cell reactivities that likely contribute to the autoimmune
- 23 response initiation<sup>10</sup>.
- Neuropathological and PET studies in anti-IgLON5 disease patients highlight the presence of
- 25 inflammation, neuronal loss and hyperphosphorylated tau deposition, with preferential
- 26 involvement of the brainstem and hypothalamus<sup>1,11-14</sup>. While there is evidence of cellular
- dysfunction and atrophy in murine models<sup>6-9,15-17</sup>, in vivo evidence from anti-IgLON5 disease
- 28 patients remains scarce, with only individual MRI studies indicating atrophy of the cerebellum,

1 cortex, midbrain	and
--------------------	-----

- 2 brainstem<sup>18-22</sup>.
- 3 Understanding atrophy patterns may help better understand the pathophysiological mechanisms of
- 4 neurological diseases and their progression, and provide quantitative measures to evaluate the
- 5 efficacy of therapeutic interventions<sup>23</sup>. For example, studies on anti-NMDA receptor (NMDAR)
- 6 encephalitis<sup>24</sup> and anti-LGI1 encephalitis<sup>25</sup> identified links between cognitive deficits and
- 7 hippocampal structural damage that could partially be prevented by early immunotherapy in the
- 8 latter disease<sup>26</sup>. In anti-IgLON5 disease, it still remains elusive whether atrophy is frequent, and if
- 9 it associates with genotype, treatment or distinct clinical manifestations.
- Here, we investigate brain atrophy patterns in anti-IgLON5 disease using MRI in the largest
- established cohort, to date. We assess the association between the development and evolution of
- 12 atrophy and distinct clinical manifestations, HLA-predispositions, disease progression, and
- immunotherapies. Ultimately, this approach provides insights into the anatomical pathophysiology
- 14 underlying this condition, as well as generating quantitative measurements of value in future
- 15 clinical trials.

# Materials and methods

### 17 Collection of Patient MRI and Clinical Data

- 18 A literature search was conducted to identify patients with anti-IgLON5 disease, and
- 19 corresponding authors and centers were contacted to request patient data. A total of 257
- 20 retrospective brain MRI datasets were collected from a multi-centre cohort of 127 patients with
- anti-IgLON5 disease (Figure 1). Patients were recruited from Germany (n = 39), France (n = 37),
- USA (n = 15), the Netherlands (n = 13), Spain (n = 6), Switzerland (n = 5), Austria (n = 4), Italy
- 23 (n = 4), Brazil (n = 1), Slovakia (n = 1), Japan (n = 1) and Denmark (n = 1) (Figure 1A). All
- patients tested positive for anti-IgLON5 antibodies in serum and/or CSF: 98% (113/115) tested
- positive in serum, 88% (98/112) tested positive in CSF and 84% (84/100) tested positive in both.
- The study was performed according to the Declaration of Helsinki and all enrolled patients or their
- 27 legal representatives gave written informed consent.

- 1 A total of 51 scans were excluded from analyses due to lack of compatible MRI sequences for
- 2 subcortical segmentation (n = 49), excessive head movement (n = 1) or brain tumour (n = 1),
- 3 resulting in 206 MRIs from 113 patients being carried forward for further analyses (Figure 1B).
- 4 One MRI study was available for 50.4% (57/113) of patients, and 49.6% (56/113) of patients had
- 5 MRI data from two or more follow-ups (for details, see Figure 1C(iv)), with varying durations
- 6 between scans (Figure 1C(v)). Scans were available from various disease stages (Figure 1C(ii) and
- 7 the median time between onset of the disease and the first brain MRI study was 25 (IQR: 9.0-53.5)
- 8 months (Figure 1C(iii)).
- 9 Clinical data were available from 107/113 (94.7%) patients (Figure 1B, 2 and 3) and were collected
- 10 from medical records and physician questionnaires<sup>4</sup>. Patients were classified according to the
- major anti-IgLON5 disease clinical manifestations, i.e. sleep disorder (parasomnia, stridor, sleep
- 12 apnea), bulbar syndrome (dysarthria, dysphagia, vocal cord paralysis), movement disorders
- 13 (chorea, bradykinesia, cerebellar ataxia, dystonia, rigidity, tremor, myoclonus), neuromuscular
- manifestations (weakness, fasciculations), cognitive impairment (memory deficits, executive
- 15 dysfunction), ocular motor abnormalities (gaze palsy, ptosis) and/or other symptoms
- 16 (neuropsychiatric symptoms, autonomic dysfunction, vestibular dysfunction, epileptic seizures),
- as previously reported<sup>3,18,27,28</sup>. Onset symptoms were defined as the initial clinical manifestations
- at symptom onset, whereas any symptoms that patients developed later over the disease course
- were classified as progression symptoms. Clinical data at the time of individual brain MRI events
- were available for 74.8% (80/107) of patients (Figure 1B), whereby 63.1% (89/141) of their scans
- 21 were recorded while patients were (still) untreated, and 36.9% (52/141) of scans after patients had
- 22 received immunotherapy (Figure 1C(i)).

### **Control Participants**

- Neuroimaging data of cognitively normal control participants were obtained from the
- Alzheimer's Disease Neuroimaging Initiative (ADNI) database (adni.loni.usc.edu) (n = 957) and
- 26 the Open Access Series of Imaging Studies<sup>29</sup> (OASIS, http://www.oasis-brains.org) (n = 423)
- 27 (Supplementary Figure 1).

### 1 Pre-processing and Volumetry Segmentation of MRI Data

- 2 Volumetric segmentation was performed with the FreeSurfer image analysis suite<sup>30,31</sup> (Version
- 3 7.3.2). This processing stream includes steps for motion correction, intensity normalization, skull
- 4 stripping, and the labelling of cortical gyri and sulci prior to performing automated cortical and
- 5 subcortical segmentation, surface reconstruction, and volumetric analysis. For the analysis of
- 6 disease-progression dependent changes in volumetry, the FreeSurfer longitudinal stream was
- 7 employed<sup>32</sup>. Importantly, this pipeline reduces the impact of inter-individual morphological
- 8 variability by employing each subject as their own control. Further, the deep-learning tool
- 9 HypothalamicSubunits<sup>33</sup> was employed to segment the hypothalamus and attain its volumetric
- estimate, and the toolbox BrainstemSubstructures<sup>34</sup> was used to segment the medulla oblongata,
- pons and midbrain. Outputs were visually inspected in FreeView. This study was hypothesis
- driven, focussing on investigating volumetry of a subset of subcortical structures that were
- previously reported to be affected by pathological alterations in anti-IgLON5 disease on the basis
- of neuropathological<sup>1,11,13</sup> and PET<sup>12,35</sup> studies, namely hypothalamus, accumbens, brainstem,
- putamen, caudate, pallidum, hippocampus, thalamus and amygdala, as well as whole brain
- 16 volume and ventricular size.

17

### Statistical Analyses

- We report median and interquartile range (IQR) for continuous variables, absolute and relative
- 19 frequencies for categorical variables, stratified by patient groups, where meaningful. Continuous
- variables are displayed using histograms, boxplots and density curves, categorical variables using
- 21 pie charts and stacked barcharts, and raw data using individual data points. Co-occurrence of
- 22 clinical manifestations are displayed using a network diagram.
- 23 A Mann-Whitney U test was used to assess the difference in age at disease onset between HLA-
- 24 DQB1\*05:~-carriers and non-carriers. A Wilcoxon signed-rank test was used to assess the
- 25 difference in frequency of clinical manifestations at symptom onset versus progression. MRI
- 26 studies of 206 control participants were age- and sex matched to patients at a 1:1 ratio<sup>36</sup>
- 27 (Supplementary Figure 1) for analyses using FreeSurfer recon-all, brainstem substructures and
- 28 hypothalamus. Linear mixed-effects models (LMM) were fitted to analyse trends and differences
- 29 in atrophy patterns<sup>37,38</sup>. The effects of sex, age at visit (fixed effects) and repeat measures in the
- 30 same individual (random intercept) were controlled for in all analyses. Especially in longitudinal

- 1 studies, controlling for age allowed for the determination of age-independent, disease-progression-
- 2 dependent volume loss. Moreover, individual analyses were further controlled for the effects of
- 3 HLA, disease progression, distinct clinical manifestations and treatment. Details on the exact
- 4 parameter specifications (fixed effects, interaction terms, random intercepts, detailed descriptions
- 5 of datasets used) of all LMM analyses are provided in Supplementary Table 1. Where multiple
- 6 comparisons across different brain structures were performed, Benjamini-Hochberg (BH) adjusted
- 7 p-values are reported. P-values are explicitly marked as either unadjusted  $(P_{unadj})$  or adjusted  $(P_{adj})$
- 8 ). All analyses were carried out in Python and R.

#### 9 Visualisations

- 10 Visualisations were prepared using Python, R, Keynote, SankeyMatic, WorldMap and FreeSurfer.
- 11 In Figure 7, data for the visualisation of IgLON5 expression was attained from the Human Protein
- 12 Atlas<sup>39</sup> (proteinatlas.org, ENSG00000142549). Data for the visualisation of IgG deposition was
- attained from Berger-Sieczkowski et al., (2023)<sup>13</sup> and data for the visualisation of tau pathology
- 14 from Gelpi et al., (2016)<sup>11</sup>, Schöberl et al., (2018)<sup>12</sup>, Theis et al., (2023)<sup>35</sup>, Berger-Sieczkowski et
- 15 al.,  $(2023)^{13}$ , Gelpi et al.,  $(2024)^{40}$  and Fan et al.,  $(2025)^{41}$ .

### 16 Results

# 17 Patient Demographics and HLA Characteristics

- In our study, 54.9% (n = 62/113) of anti-IgLON5 disease patients were male (Figure 2A). The
- median age of symptom onset was 64.0 (IQR: 58.0-70.8) years (Figure 2B(i)), and 69.0 (IQR:
- 20 61.8-75.3) years (Figure 2B(ii)) at diagnosis. Hence, the time lag between symptom onset and
- 21 diagnosis was a mean of 3.8 years (median of 24.5 months, IQR = 11.8-56.5 months) (Figure 2C).
- 22 HLA-DOB1 status available from 42 patients and showed that 76.2% (32/42 patients) carried HLA-
- 23  $DQB1*05:\sim$  (Figure 2D(i)), which was also associated with a significantly younger age at disease
- onset (mean difference = 9.7 years, P = 0.014) compared to non-HLA-DOB1\*05:~-carriers (Figure
- 25 2D(ii-iii)).

### 1 Clinical Evolution in anti-IgLON5 Disease

2 In descending order of frequencies, the most prominent manifestations at onset were bulbar syndrome (33.6%, 36/107 patients), sleep disorder (26.2%, 28/107) and movement disorders 3 (25.2%, 27/107) (Figure 3A). The number and frequency of symptoms increased during disease 4 progression in the majority of patients, whereby sleep disorders were then present in 82.2% 5 (88/107) of patients, followed by movement disorders (70.1%, 75/107) and bulbar syndrome 6 (72.9%, 78/107). Interestingly, the frequency of neuromuscular manifestations did not change 7 significantly between symptom onset (20.6%) and later disease stages (27.1%) (Figure 3A). In line 8 with these symptom trajectories, 59.8% (64/107) of patients experienced symptoms of only a 9 10 single major clinical manifestation at initial disease presentation (Figure 3B and C, top), with few reporting concurrent onset of multiple symptoms. Subsequently, the number of symptoms 11 increased over the course of disease progression, with 92.5% (99/107) experiencing symptoms of 12 13 two or more major clinical manifestations (Figure 3B and C, bottom). Further, the most common 14 co-occurrence of features at initial disease presentation was a bulbar syndrome with sleep and cognitive impairments (Figure 3C-D(i), Supplementary Table 2). During subsequent progression, 15 more co-occurrence of all features emerged, in line with the evolution of a multi-system 16 17 phenotype<sup>4</sup> (Figure 3D(ii), Supplementary Table 3).

# Anti-IgLON5 Disease Presents with Extensive and Substructure-

# **Specific Atrophy**

18

19

20

21 To assess disease-dependent atrophy patterns, brain volumetry was compared between patients and matched controls (Supplementary Figure 1). These analyses revealed atrophy of several 22 23 subcortical structures in patients compared to controls, most prominently hypothalamus (volume -26.8% [95% CI: -30.0%, -23.6%],  $P_{unadj} = 5.0 \times 10^{-39}$ ,  $P_{adj} = 5.5 \times 10^{-38}$ ), accumbens (volume -24 13.4% [95% CI: -18.3%, -8.5%],  $P_{unadj} = 1.9 \times 10^{-7}$ ,  $P_{adj} = 5.2 \times 10^{-7}$ ), brainstem (-12.1% [CI: -25 26 15.0%, -9.2%],  $P_{unadj} = 2.2 \times 10^{-14}$ ,  $P_{adj} = 1.2 \times 10^{-13}$ ), putamen (-9.1% [CI: -12.2%, -5.9%],  $P_{unadj}$  $= 6.1 \times 10^{-8}, P_{adj} = 2.2 \times 10^{-7}$ ), caudate (-7.8% [CI: -11.1%, -4.5%],  $P_{unadj} = 6.0 \times 10^{-6}, P_{adj} = 1.1$ 27  $x 10^{-5}$ ), pallidum (-5.1% [CI: -8.6%, -1.7%],  $P_{unadj} = 3.9 \times 10^{-3}$ ,  $P_{adj} = 5.3 \times 10^{-3}$ ), hippocampus (-28 5.0% [CI: -7.7%, -2.4%],  $P_{unadj} = 2.3 \times 10^{-4}$ ,  $P_{adj} = 3.7 \times 10^{-4}$ ) and thalamus (-3.8% [CI: -7.0%, -29

- 1 0.7%],  $P_{unadj} = 1.8 \times 10^{-2}$ ,  $P_{adj} = 2.2 \times 10^{-2}$ ) (Figure 4). Further segmentation of the brainstem
- 2 revealed the most prominent atrophy in the medulla (volume -20.9% [95% CI: -23.7%, -18.1%],
- 3  $P_{unadj} = 1.5 \times 10^{-33}, P_{adj} = 4.5 \times 10^{-33}$ , followed by the pons (volume -8.0% [95% CI: -10.8%, -
- 4 5.2%],  $P_{unadj} = 6.3 \times 10^{-8}$ ,  $P_{adj} = 9.5 \times 10^{-8}$ ) and midbrain (volume -2.7% [95% CI: -5.2%, -0.1%],
- 5  $P_{unadj} = 4.3 \times 10^{-2}$ ,  $P_{adj} = 4.3 \times 10^{-2}$ ) (Supplementary Figure 2). No significant volume reduction
- 6 was observed for the amygdala. Atrophy in the patient cohort was further associated with
- 7 significantly enlarged ventricles (36.7% [CI: 22.3%, 51.5%],  $P_{unadj} = 1.5 \times 10^{-6}$ ,  $P_{adj} = 3.2 \times 10^{-6}$ ),
- 8 but not whole brain volume reduction, consistent with a more focal atrophy pattern.

# 10 Disease Progression Exacerbates the Evolution of Selected

# Substructure-Specific Atrophy

9

- 12 Next, clinical and pathophysiological factors that might underly substructure-specific atrophy
- were investigated. First, the association between disease stage and atrophy was examined. In order
- 14 to accurately trace disease-progression-dependent changes in volumetry, subcortical segmentation
- of subjects with multiple MRI studies was conducted using the FreeSurfer longitudinal pipeline
- that allows for accurate inter-individual tracing of longitudinal volumetric changes<sup>32</sup>. Investigating
- 17 age-independent, disease-progression-dependent volume loss (Supplementary Table 1), increasing
- ventricle volume size (2.8%,  $P_{unadj} = 1.9 \times 10^{-5}$ ,  $P_{adj} = 2.1 \times 10^{-4}$ ) was observed, together with a
- trend for progressive atrophy in the brainstem (annual volume change, -0.5%,  $P_{unadj} = 0.03$ ,  $P_{adj} =$
- 20 0.14) (Figure 5). In addition, hypothalamus (-0.5%,  $P_{unadj} = 0.35$ ,  $P_{adj} = 0.48$ ), putamen (-0.4%,
- 21  $P_{unadj} = 0.11, P_{adj} = 0.36$ ), caudate (-0.5%,  $P_{unadj} = 0.12, P_{adj} = 0.36$ ), thalamus (-0.3%,  $P_{unadj} = 0.36$ )
- 22 0.21,  $P_{adj} = 0.45$ ), hippocampus (-0.3%,  $P_{unadj} = 0.26$ ,  $P_{adj} = 0.45$ ) and accumbens (-0.8%,  $P_{unadj} = 0.45$ )
- $= 0.29, P_{adj} = 0.45$ ) also showed volume reductions with increasing disease duration that were less
- pronounced and did not reach significance.

### 1 Atrophy Predilection Sites Mirror Nuclei of Symptomatic

#### 2 Manifestations

3

4

5

6

7

8

9

10

11

12

13

14

15

16

17

18

19

20

21

Next, due to the heterogenous symptomatic presentation of anti-IgLON5 disease, associations between different clinical manifestations and substructure-specific atrophy were examined (Figure 3). Extensive sub-structure-specific atrophy across all clinical subtypes was confirmed (Figure 6). Especially hypothalamus, accumbens, brainstem, putamen and caudate revealed consistent and severe atrophy across all clinical manifestations, while ventricular enlargement was also observed consistently across all clinical manifestations. However, the degree of regional-specific atrophy varied depending on the clinical presentation of patients (Figure 6, markings [1,2,3]). As such, the basal ganglia, and especially caudate, show a trend for being more severely atrophied in patients presenting with movement disorders (Figure 6, top grey marking), whereas thalamus and hippocampus were more affected in patients with cognitive impairment (Figure 6, bottom grey marking). Lastly, rarer and less specific clinical manifestations involving ocular-motor abnormalities and other symptoms generally present with milder and less focal atrophy. Neither increased co-occurence of multiple different clinical manifestations (Figure 3D, Supplementary Figure 3), nor disease progression within clinical subgroups (Supplementary Figure 4) associated with distinct atrophy patterns. Given the strong (~85%) association of anti-IgLON5 disease with HLA-DQB1\*05:~10, the effect of HLA-DQB1\*05:~ on atrophy development and evolution was assessed, but showed no consistent effects (Supplementary Figure 5). Furthermore, an exploratory analysis revealed no impact of immunotherapy on atrophy (Supplementary Table 1, Supplementary Figure 6).

22

23

24

25

26

27

28

29

### **Discussion**

This study reports the largest cohort of anti-IgLON5 disease patients to date and presents evidence of a specific brain atrophy pattern. Our results identify the brainstem as the key predilection site of atrophy, further to substructure-specific atrophy affecting the hypothalamus, accumbens, putamen, caudate, pallidum, hippocampus and thalamus, as well as increased ventricle size. Remarkably, this atrophy pattern closely mirrors IgLON5 expression<sup>39</sup>, autoantibody deposition<sup>13</sup> and sites of tau accumulation<sup>1,11-13,35,40,41</sup>. Moreover, ventricular enlargement and, to a milder

degree brainstem atrophy, exacerbate with disease progression. Lastly, while sub-structurespecific atrophy presents across all clinical subtypes, basal ganglia show a trend for being more severely affected in patients presenting with movement disorders, and thalamus and hippocampus in patients with cognitive impairment. Taken together, our findings provide important insights into atrophy patterns and evolution in anti-IgLON5 disease, bridging in vivo patient data with neuropathological and molecular studies, and thus have relevant implications for the pathophysiological understanding, diagnosis and treatment monitoring of anti-IgLON5 disease. Demographic and clinical presentation of patients in our study corroborate several previous observations<sup>2,4,10</sup>, specifically (i) a late age at disease onset, (ii) substantial time lag between symptom onset and disease diagnosis and (iii) overrepresentation of *HLA-DQB1\*05*:~ in patients that is associated with a shift in age at disease onset. Moreover, we observed a shift from an oligosymptomatic presentation at disease onset to a multi-system phenotype during later disease stages, with an accordingly marked increase in the prevalence of most symptoms. Interestingly, neuromuscular symptoms were an exception and remained at a relatively modest level, potentially suggesting a distinct disease mechanism or subtype within the broader condition. Our findings on the clinical presentation of patients and the co-occurrence of different manifestations bear important implications to prompt the consideration of anti-IgLON5 disease and potential testing for IgLON5 autoantibodies. Indeed, a recent study<sup>42</sup> that systematically screened plasma of subjects with idiopathic/isolated REM sleep behavior disorder (iRBD) identified that 3/339 cases presented with IgLON5 autoantibodies. Moreover, findings from Grüter et al. (2023)<sup>4</sup> revealed that a median of four physicians and frequent initial misdiagnoses are encountered by patients, prior to the correct clinical diagnosis, while our study at hand also observed an average delay of 3.8 years between onset and diagnosis. These findings highlight the need to raise awareness of anti-IgLON5 disease and its clinical presentation to facilitate early, accurate diagnosis, enabling timely treatment and improved outcomes. Our MRI analyses identified a robust and specific atrophy pattern in patients with anti-IgLON5 disease. Atrophy was shown to be substructure specific rather than affecting global brain volume, and most severely affected the hypothalamus, brainstem and accumbens, followed by putamen, caudate, pallidum, hippocampus and thalamus. Remarkably, our study shows that atrophy very closely mirrors sites of (i) high IgLON5 expression<sup>39</sup>, (ii) autoantibody deposition<sup>13</sup>, and (iii) elevated tau pathology 1,11-13,35,40,41 – i.e. MRI patterns reflect sites of immunopathological changes.

1

2

3

4

5

6

7

8

9

10

11

12

13

14 15

16

17

18

19

20

21

22

23

24

25

26

27

28

29

30

- 1 Interestingly, this contrasts with findings in other neuroimmunological diseases such as multiple
- 2 sclerosis or anti-NMDAR encephalitis that show weaker associations between routine brain MRI
- 3 patterns and proposed pathophysiological mechanisms<sup>43,44</sup>. These disorders are characterized by a
- 4 clinico-radiological paradox and only advanced imaging studies identified robust associations
- 5 between imaging alterations (e.g. functional network disruption or reduced microstructural
- 6 integrity), suggested disease mechanisms, and clinical symptoms<sup>45-47</sup>.
- 7 Our results furthermore emphasize the role of the brainstem as the predominant "pathological hub"
- 8 in anti-IgLON5 disease. Indeed, protein expression analysis showed that IgLON5 is most
- 9 abundantly expressed in the pons and medulla oblongata<sup>39</sup>, while IgG4 preferentially deposits at
- 10 the tegmentum of the brainstem, spanning the afore-mentioned structures<sup>13</sup>. Further, brainstem
- tauopathy was confirmed *in vivo* using [18F]PI-2620 PET<sup>35</sup>, Florzolotau PET<sup>41</sup> and in 15/22 cases
- studied post-mortem<sup>11,13,40</sup>. Interestingly, these studies revealed that the severity of pathology
- decreases along a caudo-cranial gradient from the medulla oblongata to the pons and the midbrain.
- Our findings reproduce the same gradient with regards to atrophy along the brainstem, whereby
- 15 the medulla was affected most severely, followed by the pons and the midbrain. Further, we
- observed an average brainstem atrophy of -12.1% in patients compared to controls, hence our
- 17 results suggest the brainstem as an *in vivo* imaging marker for tracking the progression of anti-
- 18 IgLON5 disease. Taken together, the specific atrophy pattern revealed in our study therefore
- 19 reflects previous observations from molecular and neuropathological studies.
- 20 Findings of our study also align with several previous cellular and murine studies that highlighted
- 21 neurodegenerative features in anti-IgLON5 disease, showing that IgLON5 autoantibodies cause a
- 22 decrease of surface-expressed IgLON5 clusters, impaired cellular function, elevated p-tau
- accumulation and cell death<sup>6-9,15-17</sup>. Further, studies of passive-transfer murine models<sup>9,15-17</sup>
- showed that pathogenic and inflammatory effects preferentially cluster at sites of high IgLON5
- expression. As such, tau accumulation was restricted to the brainstem, hippocampus, spinal cord
- 26 and midbrain<sup>9,15,17</sup>, and elevated astrocyte and microglial activation was reported in the
- 27 hippocampus, hypothalamus, cerebellum and midbrain<sup>9,16</sup>. This specificity was also confirmed in
- human neuropathological and PET studies, revealing an atypical 3R/4R tauopathy in the brainstem
- 29 and hypothalamus, and to a lesser degree, the hippocampus, basal ganglia, thalamus and

- 1 amygdala<sup>1,11-13,35,40,41</sup>. While similar patterns in animal models and humans are thus reflected,
- 2 further research is warranted on the transferability of murine studies to human data.
- 3 Given the progressive clinical course of anti-IgLON5 disease, we next investigated the
- 4 longitudinal development of brain atrophy patterns. We observed an age-independent, disease-
- 5 progression-dependent atrophy associated with continued ventricular enlargement and a trend for
- 6 aggravated brainstem atrophy. Importantly, these analyses were rigorously controlled for the
- 7 effects of age and inter-individual variability in subcortical volumetry, thereby ensuring a precise
- 8 assessment of the impact of disease progression on the evolution of atrophy. Indeed, our findings
- 9 align with several recent observations: First, molecular studies investigating the effects of IgLON5
- autoantibodies showed time-dependent aggravation of pathogenic effects and cell death<sup>7,8</sup>. Second,
- 11 cytotoxic tau leads to cell death and can self-propagate trans-cellularly, thus autonomously driving
- progressive atrophy in regions of high tau deposition<sup>48,49</sup>. Third, classical brainstem tauopathy
- remained absent in three cases with a short disease duration studied by Berger-Sieczkowski et al.,
- 14 (2023)<sup>13</sup>, suggesting that neurodegenerative pathology develops in a disease-progression-
- dependent manner. Taken together, previous molecular data and our longitudinal imaging analyses
- show that anti-IgLON5 disease features core hallmarks of a progressive neurodegenerative
- 17 disease.
- Further to the effect of disease progression, we studied potential correlations between substructure-
- 19 specific atrophy and the evolution of various clinical manifestations. We found that atrophy –
- 20 while present across all symptom complexes predominantly affects structures functionally
- 21 related to distinct clinical manifestations more severely. As such, putamen, caudate and pallidum
- 22 with their key role in motor control and movement coordination tended to be more severely
- affected by atrophy in patients with movement disorders. These observations align with findings
- by Gao et al., (2023)<sup>17</sup>, who showed a sustained decline in motor balance associated with reduced
- 25 projection fibres and cell death in the basal ganglia of mice injected with IgLON5 autoantibodies.
- Moreover, we observed aggravated atrophy in the hippocampus and thalamus in patients with
- cognitive symptoms. Indeed, Ni et al., (2022)<sup>16</sup> showed that mice injected with IgLON5-
- autoantibodies had cognitive deficits concurrent to neurodegeneration in the CA1 region of the
- 29 hippocampus, a core structure for learning and memory. Taken together, our findings align with
- 30 previous observations and pathophysiological considerations, postulating that substructure-
- 31 specific atrophy contributes to symptom development and specificity in anti-IgLON5 disease.

Some methodological limitations of our study must be acknowledged. First, the retrospective nature of the collection of clinical MRI data leads to an intrinsic heterogeneity in imaging and follow-up intervals between patients. Despite the application of stringent LMMs to account for variability within the dataset, residual biases may persist due to factors such as heterogeneity in scanner hardware or acquisition protocols. These confounding variables warrant careful consideration in the interpretation of the findings. However, this study design permitted the collection of a large and multi-national patient cohort, which is quite challenging in rare diseases such as anti-IgLON5 disease. Second, our segmentation toolbox did not include the cerebellum, which may also be affected in the disease<sup>11,13,40,41</sup>. Future studies should also characterise atrophy of the cerebellum and other structures that are not predominantly affected by pathology (including neocortex) in order to substantiate, whether atrophy follows sites of dominant autoimmune and neurodegenerative marker deposition. Clinical phenotyping in our study considered the mere presentation of key manifestations, without accounting for variations in their severity. Gaig et al., (2024)<sup>27</sup> recently proposed a composite score (ICS) for the clinical assessment of anti-IgLON5 disease, which captures the extent and severity of various clinical manifestations. The ICS promises a superior quantification, allowing more intricate insights into the complex interplay of atrophy and clinical presentation. Finally, our study also explored possible effects of HLA-DQB1\*05:~ and immunotherapy on atrophy development, but data was only available from a limited number of subjects and results thus remained inconclusive. However, given the key influence of HLA-DQB1\*05:~ on genetic risk, age at disease onset and autoimmunity<sup>10</sup>, future studies should further investigate possible differentiations in atrophy patterns subject to associated HLA haplotypes. Moreover, recent evidence indicates improved efficacy of immunotherapy when initiated early in the disease<sup>4</sup> and thus also a potential modulatory effect of immunotherapy on the progression of neurodegeneration and associated atrophy. However, given the retrospective and heterogeneous nature of the dataset presented in the study at hand, including variability in treatment regimens, dosages, and timing relative to imaging, the ability to isolate and interpret immunotherapy-dependent effects is inherently limited.

1

2

3

4

5

6

7

8

9

10

11

12

13

14

15

16

17

18

19

20

21

2223

24

25

26

27

28

29

30

31

Taken together, our study provides important contributions to the pathophysiological understanding, clinical monitoring and treatment of anti-IgLON5 disease. First, our findings extend the pathophysiological brain map of anti-IgLON5 disease by highlighting extensive and progressive atrophy at autoimmune and tau predilection sites. Remarkably, we identified a very

- close spatial matching between causal pathophysiologic processes including antibody and tau deposition, and brain atrophy. Second, these findings should stimulate further research into the molecular drivers of atrophy to derive effective therapeutic strategies to prevent its development and progression. Third, our findings imply that atrophy could serve as a valuable marker for disease progression and clinical phenotyping of patients. Our results thereby call for the prompt incorporation of atrophy measurements into routine clinical assessments to monitor disease
- 7 trajectory and inform improved treatment strategies.

9

# Data availability

Raw data are available on request to the corresponding author.

11

12

# Acknowledgements

- Data were provided in part by OASIS-1: Cross-Sectional: Principal Investigators: D. Marcus, R,
- 14 Buckner, J, Csernansky J. Morris; P50 AG05681, P01 AG03991, P01 AG026276, R01 AG021910,
- 15 P20 MH071616, U24 RR021382. Data collection and sharing for the Alzheimer's Disease
- Neuroimaging Initiative (ADNI) is funded by the National Institute on Aging (National Institutes
- of Health Grant U19 AG024904). The grantee organization is the Northern California Institute for
- 18 Research and Education. In the past, ADNI has also received funding from the National Institute
- 19 of Biomedical Imaging and Bioengineering, the Canadian Institutes of Health Research, and
- 20 private sector contributions through the Foundation for the National Institutes of Health (FNIH).
- 21 The Mayo Clinic Center for Multiple Sclerosis and Autoimmune Neurology.

22

23

# **Funding**

- 24 Selina M Yogeshwar received funding from the Einstein Center for Neurosciences Berlin (Einstein
- 25 Foundation Berlin) and the German-Academic Exchange Service (DAAD). Frederik Bartels is
- supported by the US National Multiple Sclerosis Society (NMSS) and was a participant in the
- 27 BIH-Charité Clinician Scientist Program funded by the Charité- Universitätsmedizin Berlin and

the Berlin Institute of Health. Christian Geis received funding from the German Research 1 Foundation (FOR3004; GE2519/8-1, GE2519/9-1 and GE2519/11-1) and the German Federal 2 3 Ministry of Education and Research (01GM1908B). Nico Melzer received funding from the 4 Bundesministerium für Bildung und Forschung, CONNECT-GENERATE 2.0 5 Aufklärung, Kategorisierung und Behandlung Forschungsverbund autoimmuner zur 6 Hirnentzündungen und verwandter Erkrankungen (01GM2208). The preparation of this article and 7 the research presented herein were supported by grants from the German Federal Ministry of 8 Education and Research (CONNECT-GENERATE grant no. 01GM1908A and 01GM2208). Frank Leypoldt is also supported by E-Rare Joint Transnational research support (ERA-Net, 9 10 LE3064/2-1), Stiftung Pathobiochemie of the German Society for Laboratory Medicine and HORIZON MSCA 2022 Doctoral Network 101119457 — IgG4-TREAT. Lidia Sabater received 11 12 funding through the Instituto de Salud Carlos III, PI21/00165. Josep Dalmau received funding through the Fundació Clínic per a la Recerca Biomedica (FCRB) Programa Multidisciplinar de 13 Recerca; Generalitat de Catalunya, Department of Health, SLT028/23/000071; CaixaResearch 14 Health 2022, HR22-00221 (JD), and Centro de Investigaciones en Red de Enfermedades Raras 15 16 (CIBERER). Harald Prüss received funding from the BMBF ('Connect Generate' 16GW0279K), 17 the Helmholtz Association (HIL-A03), the DFG (clinical research unit 5023/1 'BECAUSE-Y', PR 1274/9–1, and research unit FOR3004). Romana Hoftberger received funding from the Austrian 18 Science Fund (FWF), project number I6565-B (SYNABS). Bettina Schreiner received funding 19 20 through the Betty and David Koetser Foundation. Andrew McKeon received funding through the 21 NIH, RO1NS126227. Jan Lewerenz received funding through the German Federal Ministry of Education and Research (BMBF, CONNECT-GENERATE, 01GM1908B und 01GM2208B). 22 23 Sarosh Irani: this research was funded in whole or in part by clinical fellowships from the Medical Research Council [MR/V007173/1 and MR/X022013/1], Wellcome Trust [104079/Z/14/Z and 24 25 102176/Z/13/Z], BMA Research Grants- Vera Down grant (2013) and Margaret Temple (2017), Epilepsy Research UK (P1201), the Fulbright UK-US commission (MS-Society research award), 26 27 Association of British Neurologists and Guarantors of Brain, University of Oxford, the National 28 Institute for Health Research (NIHR) and Oxford Biomedical Research Centre (OBRC). For the 29 purpose of Open Access, the author has applied a CC BY public copyright licence to any Author Accepted Manuscript (AAM) version arising from this submission. The views expressed are those 30 of the author(s) and not necessarily those of the NHS, the NIHR or the Department of Health. 31

Emmanuel Mignot received funding through U01 NS120885. Maarten J Titulaer received funding 1 2 from the Netherlands Organization for Scientific Research (NWO, Veni incentive), ZonMw 3 (Memorabel program), the Dutch Epilepsy Foundation (NEF 14-19 & 19-08), Dioraphte (2001 0403), the Erasmus Trustfonds and E-RARE JTC 2018 (UltraAIE, 90030376505). The French 4 5 cohort of IgLON5 encephalitis is part of the BETPSY project, which is supported by a public grant overseen by the Agence Nationale de la Recherche (ANR; French research agency) as part of the 6 Investissements d'Avenir program (ANR-18-RHUS-0012), also performed within the framework 7 8 of the LABEX CORTEX of the Universitè Claude Bernard Lyon 1 (program Investissements d'Avenir, ANR-11-LABX-0042, operated by the ANR) and supported by the European Reference 9 Network RITA. Carsten Finke received funding from the Deutsche Forschungsgemeinschaft 10 (DFG, German Research Foundation), grant numbers 327654276 (SFB 1315), 504745852 11 12 (Clinical Research Unit KFO 5023 'BecauseY'), FI 2309/1-1 (Heisenberg Program) and FI 2309/2-1; and the German Ministry of Education and Research (BMBF), grant number 01GM2208C 13 (CONNECT-GENERATE). 14

16 Competing interests

- 17 Marius Ringelstein received speaker honoraria from Novartis, Bayer Vital GmbH, Roche,
- 18 Alexion, Horizon/Amgen and Ipsen and travel reimbursement from Bayer Schering, Biogen
- 19 Idec, Merz, Genzyme, Teva, Roche, Alexion, Horizon/Amgen and Merck, none related to this
- study. Anastasia Zekeridou has patents pending on PDE10A-IgG, CAMKV-IgG, DACH1-IgG,
- 21 Tenascin-R-IgG as markers of paraneoplastic autoimmunity and received research funding from
- 22 Roche/Genentech, of which none is relevant to this project. Frank Leypoldt discloses speaker
- 23 honoraria from Grifols, Teva, Biogen, Bayer, Roche, Novartis, Fresenius, travel funding from
- 24 Merck, Grifols and Bayer and serving on advisory boards for Roche, Biogen, Argenx and
- 25 Alexion. Francesc Graus receives royalties from Euroimmun for the use of IgLON5 as an
- 26 autoantibody test and honoraria for Associate Editor of MedLink Neurology. Sean Pittock has
- 27 received personal compensation for serving as a consultant for Roche/Genentech, Sage
- 28 Therapeutics, Arialys and Astellas. He's received personal compensation for serving on
- 29 scientific advisory boards or data safety monitoring boards for F. Hoffman-LaRoche AG,
- 30 Genentech, Arialys and UCB. His institution has received compensation for serving as a

- 1 consultant for Astellas, Alexion, and Viela Bio/MedImmune. All compensation is paid to Mayo
- 2 Clinic. He has received research support from Alexion, Viela Bio/MedImmune,
- 3 Roche/Genentech and Adimmune. He has a patent, Patent# 8,889,102 (Application#12-678350,
- 4 Neuromyelitis Optica Autoantibodies as a Marker for Neoplasia)—issued; a patent, Patent#
- 5 9,891,219B2 (Application#12-573942, Methods for Treating Neuromyelitis Optica (NMO) by
- 6 Administration of Eculizumab to an individual that is Aquaporin-4 (AQP4)-IgG Autoantibody
- 7 positive)-issued and from which he has received royalties and a patent for GFAP-IgG; Septin-5-
- 8 IgG; MAP1B-IgG; Kelch-like protein 11; PDE10A pending. He is working as a consultant in the
- 9 Mayo Clinic Neuroimmunology laboratory clinical service. The Mayo Clinic Neuroimmunology
- 10 Laboratory commercially offers MOG-IgG testing, but revenue accrued does not contribute to
- salary, research support, or personal income. Josep Dalmau receives royalties from Euroimmun
- for the use of NMDA as an antibody test. He received a licensing fee from Euroimmun for the
- use of GABAB receptor, GABAA receptor, DPPX and IgLON5 as autoantibody tests; he has
- 14 received a research grant from Sage Therapeutics. Romana Höftberger reports honoraria from
- 15 UCB. The Medical University of Vienna (Austria; employer of Prof. Höftberger) receives
- payment for antibody assays and for antibody validation experiments organized by Euroimmun
- 17 (Lübeck, Germany). Andrew McKeon patents issued for GFAP and MAP1B-IgGs and patents
- pending for Septins-5 and -7 and KLCHL11-IgGs, and has consulted for Roche pharmaceuticals,
- 19 without personal compensation. Jan Lewerenz reports travel honoraria and speaker's fees from
- 20 the Cure Huntington's Disease Initiative (CHDI), the Movement Disorders Society as the
- 21 German Society for Cerebrospinal Fluid Diagnostic and Clinical Neurochemistry (DGLN),
- 22 Alexion, Biogen, Sanofi, Teva, Merck, Novartis, Janssen, Fujirebio, Roche, and Neuraxpharm.
- His institution received financial compensation for clinical trials with Jan Lewerenz as principal
- 24 investigator from CHDI and SOM Biotech. He is member of the executive board of the DGLN
- 25 (Deutsche Gesellschaft für Liquordiagnostik und klinische Neurochemie, German Society for
- 26 Cerebrospinal Fluid Diagnostics and Clinical Neurochemistry). He received research funding
- 27 from the German Federal Ministry of Education and Research (BMBF, CONNECT-
- 28 GENERATE, 01GM1908B und 01GM2208B) and the Boehringer Ingelheim University
- 29 Biocenter. Sarosh Irani has received honoraria/research support from UCB, Immunovant,
- 30 MedImmun, Roche, Janssen, Cerebral therapeutics, ADC therapeutics, Brain, CSL Behring, and
- 31 ONO Pharma, and receives licensed royalties on patent application WO/2010/046716 entitled

- 1 'Neurological Autoimmune Disorders', and has filed two other patents entitled "Diagnostic
- 2 method and therapy" (WO2019211633 and US app 17/051,930; PCT application
- 3 WO202189788A1) and "Biomarkers" (WO202189788A1, US App 18/279,624;
- 4 PCT/GB2022/050614). Maarten J. Titulaer has filed a patent, on behalf of the Erasmus MC, for
- 5 methods for typing neurological disorders and cancer, and devices for use therein, and has
- 6 received research funds for serving on a scientific advisory board of Horizon
- 7 Therapeutics/Amgen and Argenx, for consultation at Guidepoint Global LLC, and for
- 8 consultation at UCB. MT has received an unrestricted research grant from Euroimmun AG, and
- 9 from CSL Behring. MT receives royalties from UpToDate Inc. Carsten Finke has received
- 10 research support from Euroimmun AG and speaker honoraria from Bristol Myer Squibb, Alexion
- 11 and UCB.

13

# Supplementary material

14 Supplementary material is available at *Brain* online.

15

16

# Appendix 1

# 17 IgLON5 Imaging Consortium

- 18 Aurélie Méneret Isabelle Francillard, Dimitri Renard, Virginie Desestret, Nicolas Capet,
- 19 Jeanbaptiste Davion, Julie Boucher, Helene Zephir, Philippe Damier, Helene Combres, Marie
- 20 Rafiq, Fabrice Bonneville, Marina Cumin, Antoine Soulages, Mathilde Compoint, Maximilien
- 21 Moulin, Edouard Berling, Eve Garrigues, Marine Chanson, Veronique Bourg, Caroline Giordana,
- 22 Jeanne Benoit, Olivier Flabeau, Emmanuelle Derivoyre, Gilles Ryckewaert, Tifanie Alberto,
- Nicolas Carriere, Sohrab Mostoufizadehs, Melanie Barbay, Marie Benaiteau, Alberto Vogrig,
- 24 Francois Sellal, Olivier Casez, Cedric Bruel, L Kalifa, Elena Camelia Rusu, Sarah Demortiere,
- 25 Adil Maarouf, Adrien Wang, Adelaide Brasset, Clarisse Carra Dalliere, Arthur Attal, Céline
- 26 Demourant, Florent Cluse, Jean-Luc Houeto, Norbert Brueggemann, Justina Dargvainiene,
- 27 Thomas Seifert, Ulrich Hofstadt-van Oy, Michael Nagel, Christian Urbanek, Ina Schroeder, Peter

- 1 Schramm, Silke Tonner, Caspar Seitz, Marlene Tschernatsch, Ha-Yeun Chung, Jonathan Wickel,
- 2 Florian Schoeberl, Stefan Macher, Mateus M Simabukuro, Simone Zittel-Dirks, Brigitte
- 3 Wildemann, Jan Kothaj, Carlos Ordas, Javier Villacieros Álvarez, Klemens Angstwurm, Stefan
- 4 Macher, Evelyn Berger-Sieczkowski, Ángela Milán Tomás, Antonio Martin Bastida, Sonia
- 5 Quintas, Nicola Tambasco, Pasquale Nigro, Raffaele Iorio, Yoya Ono, Takayoshi Shimohata,
- 6 Kimura Akio, Takekoshi Akira, Mette Scheller-Nissen, Christian Hartmann, Danielle Bastiaansen,
- 7 Robin van Steenhoven and Katia Schwichtenberg.

9

# Supplementary material

10 Supplementary material is available at *Brain* online.

11

12

# References

- 13 1. Sabater L, Gaig C, Gelpi E, et al. A novel non-rapid-eye movement and rapid-eye-
- movement parasomnia with sleep breathing disorder associated with antibodies to IgLON5: a
- 15 case series, characterisation of the antigen, and post-mortem study. *The Lancet Neurology*.
- 16 2014;13(6):575-586.
- 17 2. Gaig C, Compta Y, Heidbreder A, et al. Frequency and Characterization of Movement
- Disorders in Anti-IgLON5 Disease. *Neurology*. Aug 11 2021;97(14):e1367-81.
- 19 doi:10.1212/WNL.000000000012639
- 3. Gaig C, Sabater L. New knowledge on anti-IgLON5 disease. Curr Opin Neurol. Jun 1
- 21 2024;37(3):316-321. doi:10.1097/WCO.0000000000001271
- 4. Grüter T, Möllers FE, Tietz A, et al. Clinical, serological and genetic predictors of
- response to immunotherapy in anti-IgLON5 disease. *Brain*. Feb 13 2023;146(2):600-611.
- 24 doi:10.1093/brain/awac090
- 25 5. Cabezudo-Garcia P, Mena-Vazquez N, Estivill Torrus G, Serrano-Castro P. Response to
- 26 immunotherapy in anti-IgLON5 disease: A systematic review. Acta Neurol Scand. Apr
- 27 2020;141(4):263-270. doi:10.1111/ane.13207

- 1 6. Sabater L, Planagumà J, Dalmau J, Graus F. Cellular investigations with human
- 2 antibodies associated with the anti-IgLON5 syndrome. J Neuroinflammation. Sep 1
- 3 2016;13(1):226. doi:10.1186/s12974-016-0689-1
- 4 7. Landa J, Gaig C, Plaguma J, et al. Effects of IgLON5 Antibodies on Neuronal
- 5 Cytoskeleton: A Link between Autoimmunity and Neurodegeneration. Ann Neurol. Nov
- 6 2020;88(5):1023-1027. doi:10.1002/ana.25857
- 7 8. Ryding M, Gamre M, Nissen MS, et al. Neurodegeneration Induced by Anti-IgLON5
- 8 Antibodies Studied in Induced Pluripotent Stem Cell-Derived Human Neurons. Cells. Apr 8
- 9 2021;10(4)doi:10.3390/cells10040837
- 10 9. Askin B, Cordero Gomez C, Duong SL-L, et al. Autoimmune antibody-induced neuronal
- 11 hyperactivity triggers pathological Tau in IgLON5 disease. *bioRxiv*. 2024:2024.03. 10.584272.
- 12 10. Yogeshwar SM, Muñiz-Castrillo S, Sabater L, et al. HLA-DQB1\*05 subtypes and not
- DRB1\*10:01 mediates risk in anti-IgLON5 disease. Brain. Mar 1 2024;
- 14 11. Gelpi E, Höftberger R, Graus F, et al. Neuropathological criteria of anti-IgLON5-related
- tauopathy. *Acta neuropathologica*. 2016;132:531-543.
- 16 12. Schöberl F, Levin J, Remi J, et al. IgLON5: a case with predominant cerebellar tau
- deposits and leptomeningeal inflammation. *Neurology*. 2018;91(4):180-182.
- 18 13. Berger-Sieczkowski E, Endmayr V, Haider C, et al. Analysis of inflammatory markers
- and tau deposits in an autopsy series of nine patients with anti-IgLON5 disease. *Acta*
- 20 Neuropathol. Oct 2023;146(4):631-645. doi:10.1007/s00401-023-02625-6
- 21 14. Theis H, Bischof GN, Brüggemann N, et al. In Vivo Measurement of Tau Depositions in
- 22 Anti-IgLON5 Disease Using [18F] PI-2620 PET. *Neurology*. 2023;101(22):e2325-e2330.
- 23 15. Alvente S, Matteoli G, Molina-Porcel L, et al. Pilot Study of the Effects of Chronic
- 24 Intracerebroventricular Infusion of Human Anti-IgLON5 Disease Antibodies in Mice. Cells. Mar
- 25 17 2022;11(6)doi:10.3390/cells11061024
- 26 16. Ni Y, Feng Y, Shen D, et al. Anti-IgLON5 antibodies cause progressive behavioral and
- 27 neuropathological changes in mice. *J Neuroinflammation*. Jun 11 2022;19(1):140.
- 28 doi:10.1186/s12974-022-02520-z

- 1 17. Gao Y, Li H, Luo H, et al. Purified Serum IgG from a Patient with Anti-IgLON5
- 2 Antibody Cause Long-Term Movement Disorders with Impaired Dopaminergic Pathways in
- 3 Mice. *Biomedicines*. Sep 7 2023;11(9)doi:10.3390/biomedicines11092483
- 4 18. Gaig C, Graus F, Compta Y, et al. Clinical manifestations of the anti-IgLON5 disease.
- 5 *Neurology*. 2017;88(18):1736-1743.
- 6 19. Honorat JA, Komorowski L, Josephs KA, et al. IgLON5 antibody: Neurological
- 7 accompaniments and outcomes in 20 patients. Neurol Neuroimmunol Neuroinflamm. Sep
- 8 2017;4(5):e385. doi:10.1212/NXI.000000000000385
- 9 20. Montojo T, Piren V, Benkhadra F, Codreanu A, Diederich NJ. Gaze Palsy, Sleep and
- Gait Disorder, as Well as Tako-Tsubo Syndrome in a Patient with Ig LON5 Antibodies.
- 11 *Movement disorders clinical practice*. 2017;4(3)
- 12 21. Montagna M, Amir R, De Volder I, Lammens M, Huyskens J, Willekens B. IgLON5-
- 13 Associated Encephalitis With Atypical Brain Magnetic Resonance Imaging and Cerebrospinal
- 14 Fluid Changes. Front Neurol. 2018;9:329. doi:10.3389/fneur.2018.00329
- 15 22. Urso D, De Blasi R, Anastasia A, et al. Neuroimaging Findings in a Patient with Anti-
- 16 IgLON5 Disease: Cerebrospinal Fluid Dynamics Abnormalities. *Diagnostics (Basel)*. Mar 30
- 17 2022;12(4)doi:10.3390/diagnostics12040849
- 18 23. Hartung TJ, Bartels F, Kuchling J, et al. MRI findings in autoimmune encephalitis. *Revue*
- 19 *Neurologique*. 2024;doi:https://doi.org/10.1016/j.neurol.2024.08.006
- 20 24. Finke C, Kopp UA, Pajkert A, et al. Structural Hippocampal Damage Following Anti-N-
- 21 Methyl-D-Aspartate Receptor Encephalitis. *Biol Psychiatry*. May 1 2016;79(9):727-734.
- doi:10.1016/j.biopsych.2015.02.024
- 23 25. Finke C, Pruss H, Heine J, et al. Evaluation of Cognitive Deficits and Structural
- 24 Hippocampal Damage in Encephalitis With Leucine-Rich, Glioma-Inactivated 1 Antibodies.
- 25 JAMA Neurol. Jan 1 2017;74(1):50-59. doi:10.1001/jamaneurol.2016.4226
- 26 26. Irani SR, Stagg CJ, Schott JM, et al. Faciobrachial dystonic seizures: the influence of
- immunotherapy on seizure control and prevention of cognitive impairment in a broadening
- 28 phenotype. *Brain*. Oct 2013;136(Pt 10):3151-62. doi:10.1093/brain/awt212

- 1 27. Gaig C, Grüter T, Heidbreder A, et al. Development of a Composite Score for the
- 2 Clinical Assessment of Anti-IgLON5 Disease. *Neurology*. Apr 9 2024;102(7):e208101.
- 3 doi:10.1212/wnl.0000000000208101
- 4 28. Ono Y, Kimura A, Shimohata T. Pathogenesis, clinical features and treatment of anti-
- 5 IgLON5 disease. Clinical and Experimental Neuroimmunology. 2023;14(4):167-174,
- 6 doi:10.1111/cen3.12759
- 7 29. Marcus DS, Wang TH, Parker J, Csernansky JG, Morris JC, Buckner RL. Open Access
- 8 Series of Imaging Studies (OASIS): cross-sectional MRI data in young, middle aged,
- 9 nondemented, and demented older adults. Journal of cognitive neuroscience. 2007;19(9):1498-
- 10 1507.
- 11 30. Fischl B. FreeSurfer. *Neuroimage*. 2012;62(2):774-781.
- 12 31. Iglesias JE, Billot B, Balbastre Y, et al. SynthSR: A public AI tool to turn heterogeneous
- clinical brain scans into high-resolution T1-weighted images for 3D morphometry. Sci Adv. Feb
- 14 3 2023;9(5):eadd3607. doi:10.1126/sciadv.add3607
- 15 32. Reuter M, Schmansky NJ, Rosas HD, Fischl B. Within-subject template estimation for
- unbiased longitudinal image analysis. *Neuroimage*. 2012;61(4):1402-1418.
- 17 33. Billot B, Bocchetta M, Todd E, Dalca AV, Rohrer JD, Iglesias JE. Automated
- segmentation of the hypothalamus and associated subunits in brain MRI. *Neuroimage*.
- 19 2020;223:117287,
- 20 34. Iglesias JE, Van Leemput K, Bhatt P, et al. Bayesian segmentation of brainstem
- 21 structures in MRI. *Neuroimage*. 2015;113:184-195.
- 22 35. Theis H, Bischof GN, Bruggemann N, et al. In Vivo Measurement of Tau Depositions in
- 23 Anti-IgLON5 Disease Using [18F]PI-2620 PET. Neurology. Nov 27 2023;101(22):e2325-e2330.
- 24 doi:10.1212/WNL.0000000000207870
- 25 36. Stuart EA, King G, Imai K, Ho D. MatchIt: nonparametric preprocessing for parametric
- 26 causal inference. Journal of statistical software. 2011;
- 27 37. Douglas Bates M, Bolker B, Walker S. Fitting linear mixed-effects models using lme4.
- 28 Journal of Statistical Software. 2015;67(1):1-48.

- 1 38. Bartels F, Krohn S, Nikolaus M, et al. Clinical and Magnetic Resonance Imaging
- 2 Outcome Predictors in Pediatric Anti-N-Methyl-D-Aspartate Receptor Encephalitis. *Ann Neurol*.
- 3 Jul 2020;88(1):148-159. doi:10.1002/ana.25754
- 4 39. Uhlén M, Fagerberg L, Hallström BM, et al. Tissue-based map of the human proteome.
- 5 Science. 2015;347(6220):1260419.
- 6 40. Gelpi E, Reinecke R, Gaig C, et al. Neuropathological spectrum of anti-IgLON5 disease
- 7 and stages of brainstem tau pathology: updated neuropathological research criteria of the disease-
- 8 related tauopathy. Acta Neuropathol. Oct 14 2024;148(1):53. doi:10.1007/s00401-024-02805-y
- 9 41. Fan S, Jia C, Liang M, et al. Patterns of Tau pathology in patients with anti-IgLON5
- disease visualized by Florzolotau (18F) PET. J Neurol. Jan 15 2025;272(2):115.
- 11 doi:10.1007/s00415-024-12874-4
- 12 42. Postuma R, Vorasoot N, St Louis EK, et al. IGLON5 Frequency in Idiopathic REM Sleep
- 13 Behavior Disorder: A Multicenter Study. Neurol Neuroimmunol Neuroinflamm. Nov
- 14 2024;11(6):e200311. doi:10.1212/NXI.0000000000200311
- Heine J, Pruss H, Bartsch T, Ploner CJ, Paul F, Finke C. Imaging of autoimmune
- encephalitis--Relevance for clinical practice and hippocampal function. *Neuroscience*. Nov 19
- 17 2015;309:68-83. doi:10.1016/j.neuroscience.2015.05.037
- 18 44. Hartung TJ, Cooper G, Junger V, et al. The T1-weighted/T2-weighted ratio as a
- 19 biomarker of anti-NMDA receptor encephalitis. J Neurol Neurosurg Psychiatry. Mar 13
- 20 2024;95(4):366-373. doi:10.1136/jnnp-2023-332069
- 21 45. Peer M, Prüss H, Ben-Dayan I, Paul F, Arzy S, Finke C. Functional connectivity of large-
- scale brain networks in patients with anti-NMDA receptor encephalitis: an observational study.
- 23 *The Lancet Psychiatry*. 2017;4(10):768-774.
- 24 46. Eijlers AJ, Wink AM, Meijer KA, Douw L, Geurts JJ, Schoonheim MM. Reduced
- 25 network dynamics on functional MRI signals cognitive impairment in multiple sclerosis.
- 26 Radiology. 2019;292(2):449-457.
- 27 47. Krohn S, Müller-Jensen L, Kuchling J, et al. 2024;doi:10.1101/2024.03.07.583948

- 1 48. Fung CW, Guo J, Fu H, Figueroa HY, Konofagou EE, Duff KE. Atrophy associated with
- 2 tau pathology precedes overt cell death in a mouse model of progressive tauopathy. Sci Adv. Oct
- 3 2020;6(42)doi:10.1126/sciadv.abc8098
- 4 49. Uemura MT, Luk KC, Lee VM, Trojanowski JQ. Cell-to-Cell Transmission
- of Tau and alpha-Synuclein. *Trends Mol Med*. Oct 2020;26(10):936-952.
- 6 doi:10.1016/j.molmed.2020.03.012

8

# Figure Legends

- 9 Figure 1 Data Collection of Anti-IgLON5 Patients. (A) Retrospective patient data was
- 10 collected from twelve countries: Germany (n = 39), France (n = 37), USA (n = 15), Netherlands
- 11 (n = 13), Spain (n = 6), Switzerland (n = 5), Austria (n = 4), Italy (n = 4), Brazil (n = 1), Slovakia
- 12 (n = 1), Japan (n = 1) and Denmark (n = 1). (B) Availability of clinical and MRI data of all
- 13 collected patients. (C) MRI data availability. (i) Number of MRI scans available relative to
- immunotherapy treatment. (ii) Number of MRI scans available relative to disease onset and
- diagnosis. (iii) Time of MRI scans relative to disease onset. (iv) Number of MRI scans available
- across patients. (v) Follow up trajectory of patients with 2 or more MRI scans and treatment
- status at time of MRI.

18

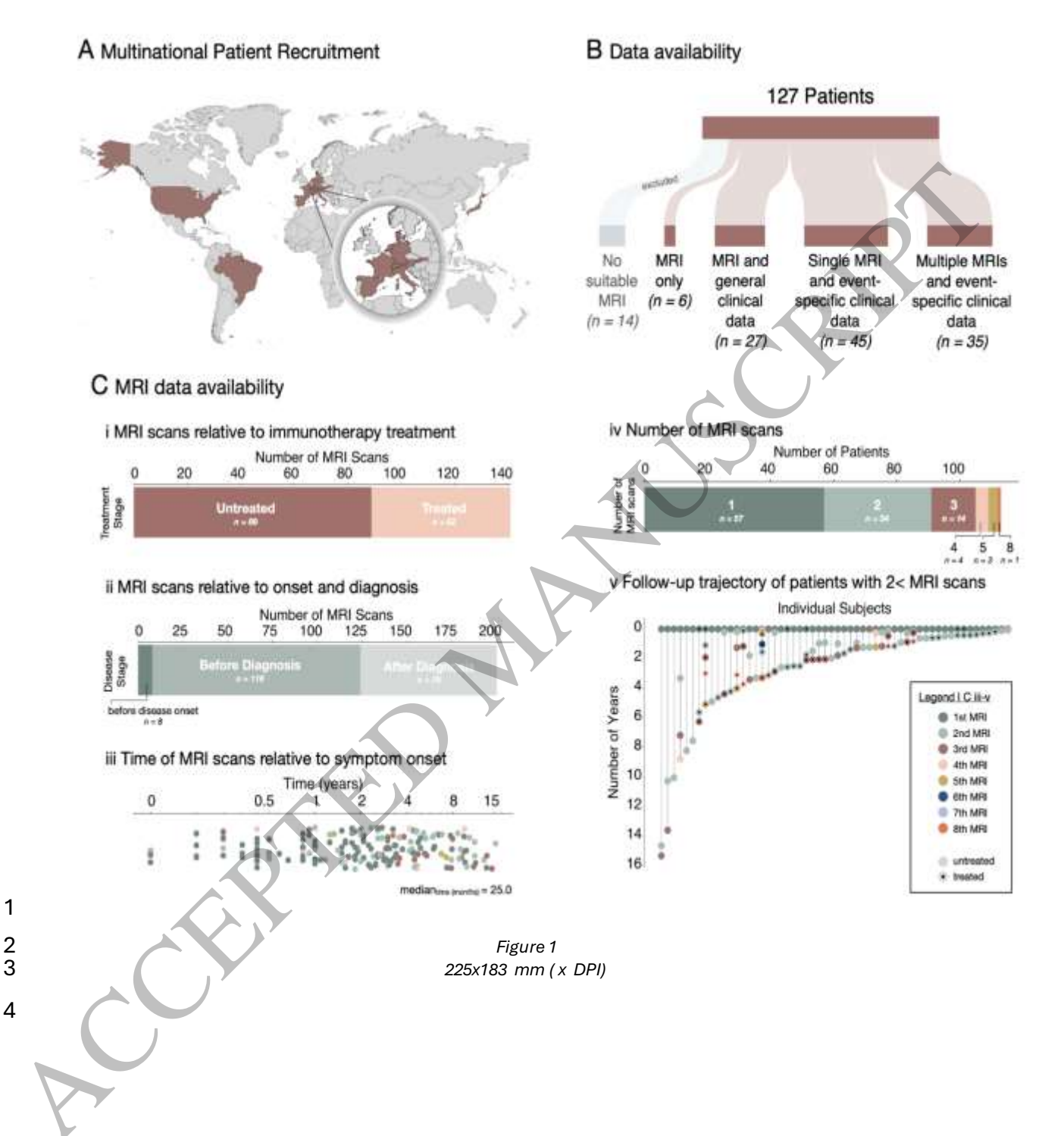
- 19 Figure 2 Demographic Presentation and HLA of Anti-IgLON5 Patients. (A) Sex distribution
- of patients. (B) Age of patients at disease (i) onset and (ii) diagnosis. (C) Time between disease
- onset and diagnosis. (D) *HLA-DOB1\*05*:~ status is known from 39.3% (42/107) subjects. (i)
- 22 Carrier frequency highlights predominance of *HLA-DQB1\*05*:~ over non-*HLA-DQB1\*05*:~. (ii)
- 23 Age at disease onset of non-HLA-DQB1\*05:~-carriers and (iii) HLA-DQB1\*05:~-carriers
- 24 highlights significantly younger age at disease onset in *HLA-DQB1\*05*:~-carriers versus non-
- 25 *HLA-DQB1\*05:*~-carriers. \* P < 0.05

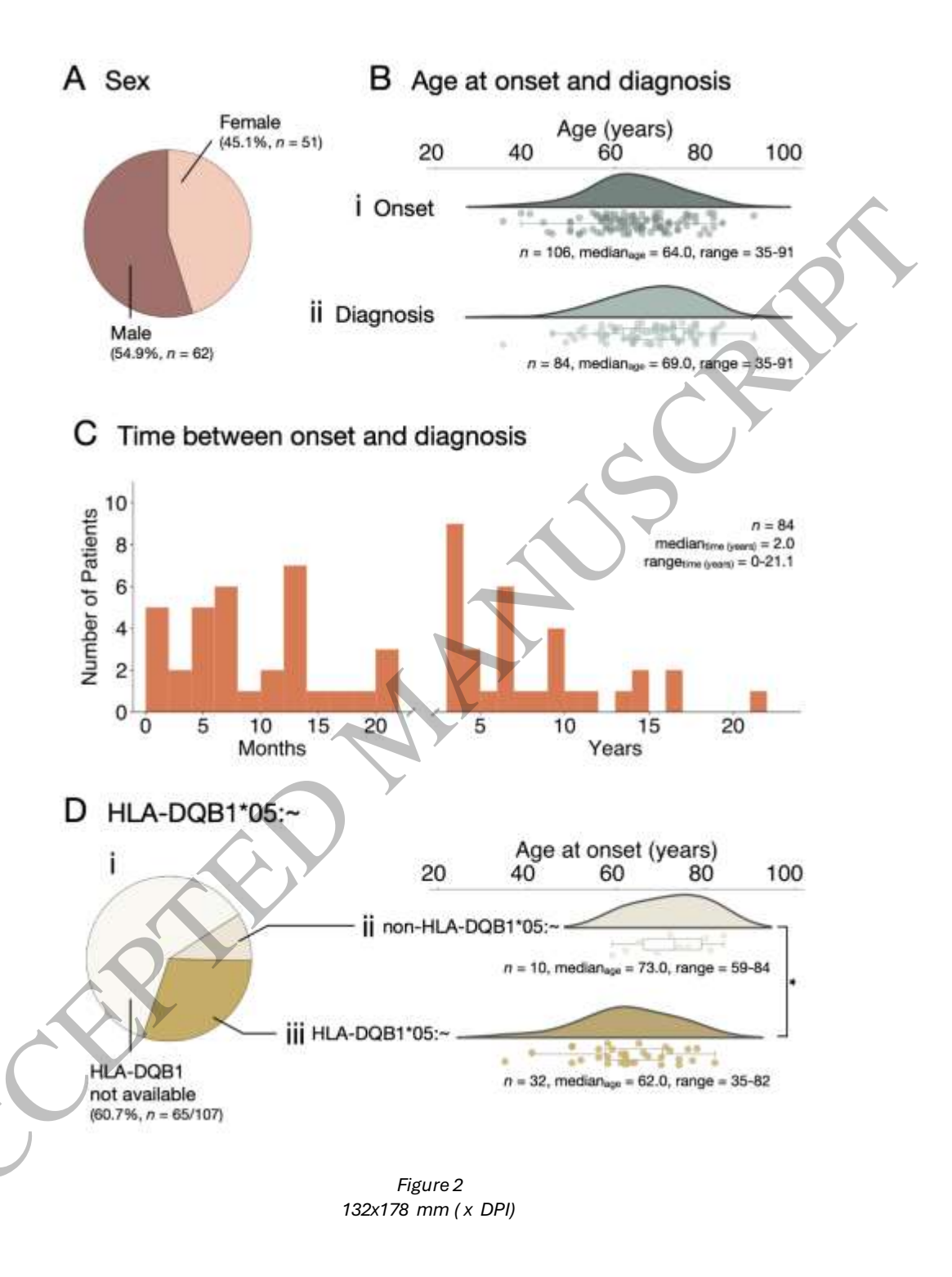
- Figure 3 Clinical Presentation of Anti-IgLON5 Patients. (A) Frequency of major clinical
- 28 manifestations (sleep disorder, bulbar syndrome, movement disorders, neuromuscular

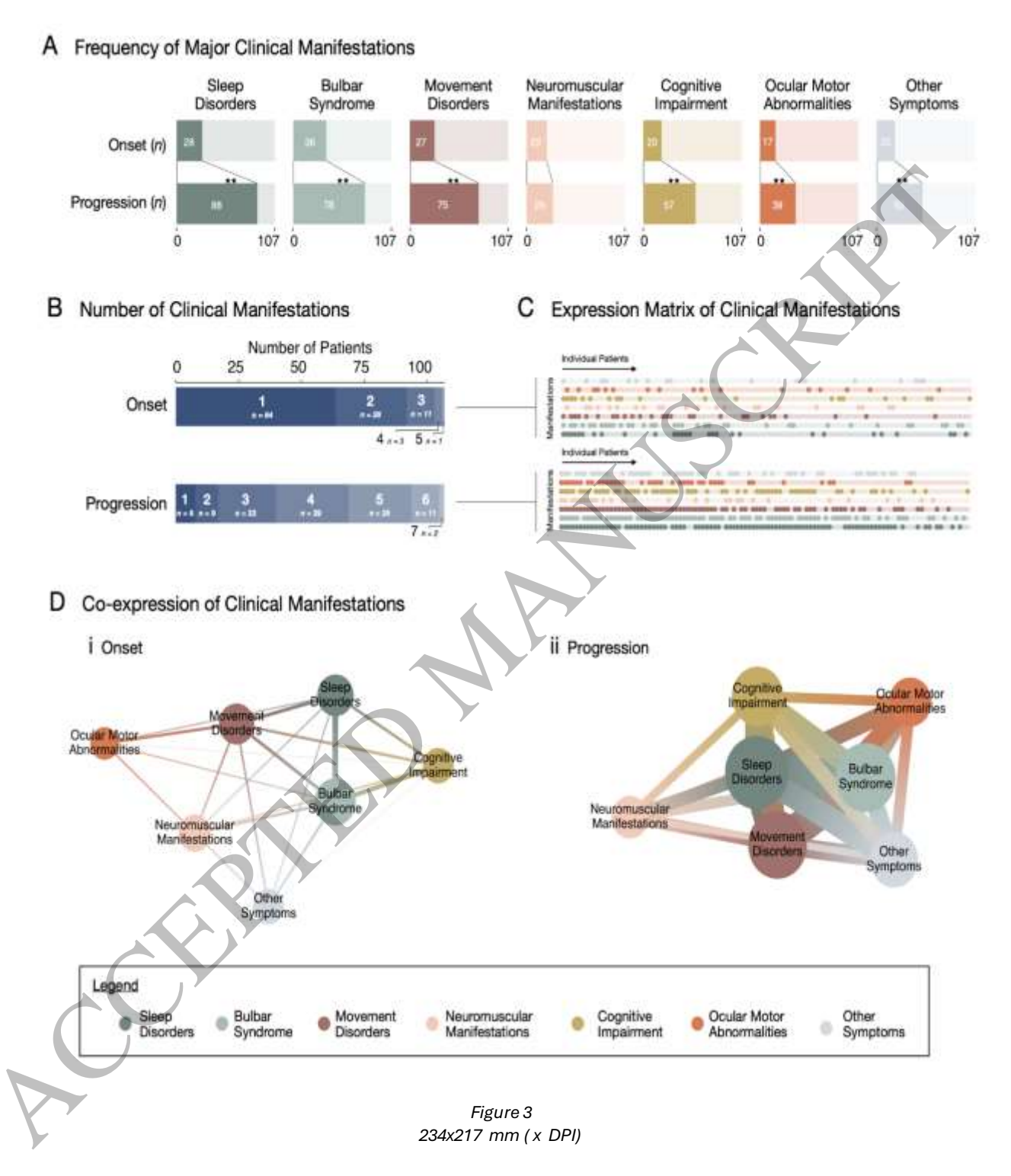
- manifestations, cognitive impairment, ocular motor abnormalities and/or other symptoms) at symptom onset and disease progression. All symptoms except for neuromuscular manifestations significantly increase in presentation over disease progression compared to symptom onset. (B) Number of major clinical manifestations at symptom onset and disease progression highlight that the majority of patients experience only a single manifestation at onset, however, develop a multi-system phenotype as the disease progresses. (C) Presentation of major clinical manifestations by each patient at symptom onset and disease progression (light hue = manifestation not present; dark hue = manifestation present). (D) Co-occurrence of major clinical manifestations with network analysis highlighting their interconnections at symptom (i) onset and (ii) progression. The size of centroids highlights the frequency of each manifestation, the connecting lines which manifestations co-occur, and the thickness of the connecting lines what the frequency of co-occurrence is. The frequency and co-occurrence of all manifestations is increased at disease progression compared to onset. \*\*P < 0.01Figure 4 Cross-Sectional Volumetry of Anti-IgLON5 Patients. (A) Anatomy of subcortical
  - Figure 4 Cross-Sectional Volumetry of Anti-IgLON5 Patients. (A) Anatomy of subcortical structures in their respective colour-coding that is carried forward in the remaining figure. (B) Region of interest (ROI) volumetry of patients (*coloured*) and matched controls (*grey*) shows significantly smaller volumetry in patients compared to controls in the hypothalamus, accumbens, brainstem, putamen, caudate, pallidum, hippocampus, thalamus, and enlarged ventricles. (C) Relative difference and 95% CI (in %) in ROI volumetry between patients and matched controls shown in (B) \*  $P_{adj} < 0.05$ . For details on parameters included in analyses, see Supplementary Table 1.

Figure 5 Longitudinal Changes in Volumetry. (A) Volumetry of ROIs (for anatomy, see Figure 4A) over disease course (= time since disease onset) in years. Scatters show raw data and black line the estimate + 95% CI of change in volumetry over the disease course. A trend for disease progression dependent reduction in the brainstem ( $P_{unadj} < 0.05$ ) is visible, as well as a significant enlargement of the ventricles ( $P_{adj} < 0.05$ ). \*  $P_{adj} < 0.05$ . [\*]  $P_{unadj} < 0.05$ . For details on parameters included in analyses, see Supplementary Table 1.

- 1 Figure 6 Relationship between Clinical Manifestations and Volumetry. (A) Relative
- 2 difference and 95% CI (in %) in ROI volumetry (for anatomy, see Figure 4A) between patients
- 3 presenting with specific clinical manifestation at the time of the MRI (Supplementary Tables 1-
- 4 3) and matched controls. Markings [1,2,3] indicate which manifestations are affected by the most
- 5 severe difference in volumetry compared to controls. Grey markings of putamen, caudate and
- 6 pallidum show that atrophy is severest in patients suffering from movement disorders. Grey
- 7 markings of hippocampus, and thalamus show that atrophy is severest in patients suffering from
- 8 cognitive impairment. For details on parameters included in analyses, see Supplementary Table
- 9 1.
- 10
- 11 Figure 7 From Autoimmunity to Neurodegeneration. (Top) Suggested molecular
- pathophysiology of anti-IgLON5 disease. IgLON5 is expressed extra-cellularly on neurons and
- targeted by IgLON5 autoantibodies. Intra-cellularly, hyperphosphorylated tau accumulates,
- 14 ultimately forming tau tangles and leading to neurodegeneration. (Bottom) Substructures
- 15 investigated in this study are shown. IgLON5 Expression: Expression of IgLON5 RNA
- according to the Human Protein Atlas<sup>39</sup> (proteinatlas.org, ENSG00000142549). IgG Deposition:
- Deposition of IgG1 and IgG4 antibodies is shown according to Berger-Sieczkowski et al.,
- 18  $(2023)^{13}$ . Tau Pathology: Distribution of tau pathology is shown according to Gelpi *et al.*,
- 19 (2016)<sup>11</sup>, Schöberl et al.,  $(2018)^{12}$ , Theis et al.,  $(2023)^{35}$ , Berger-Sieczkowski et al.,  $(2023)^{13}$ ,
- Gelpi et al.,  $(2024)^{40}$  and Fan et al.,  $(2025)^{41}$ . Atrophy: Predilection sites of atrophy
- 21 demonstrated in this study are shown. For anatomical legend of subcortical structures, please
- 22 refer to Figure 4A.







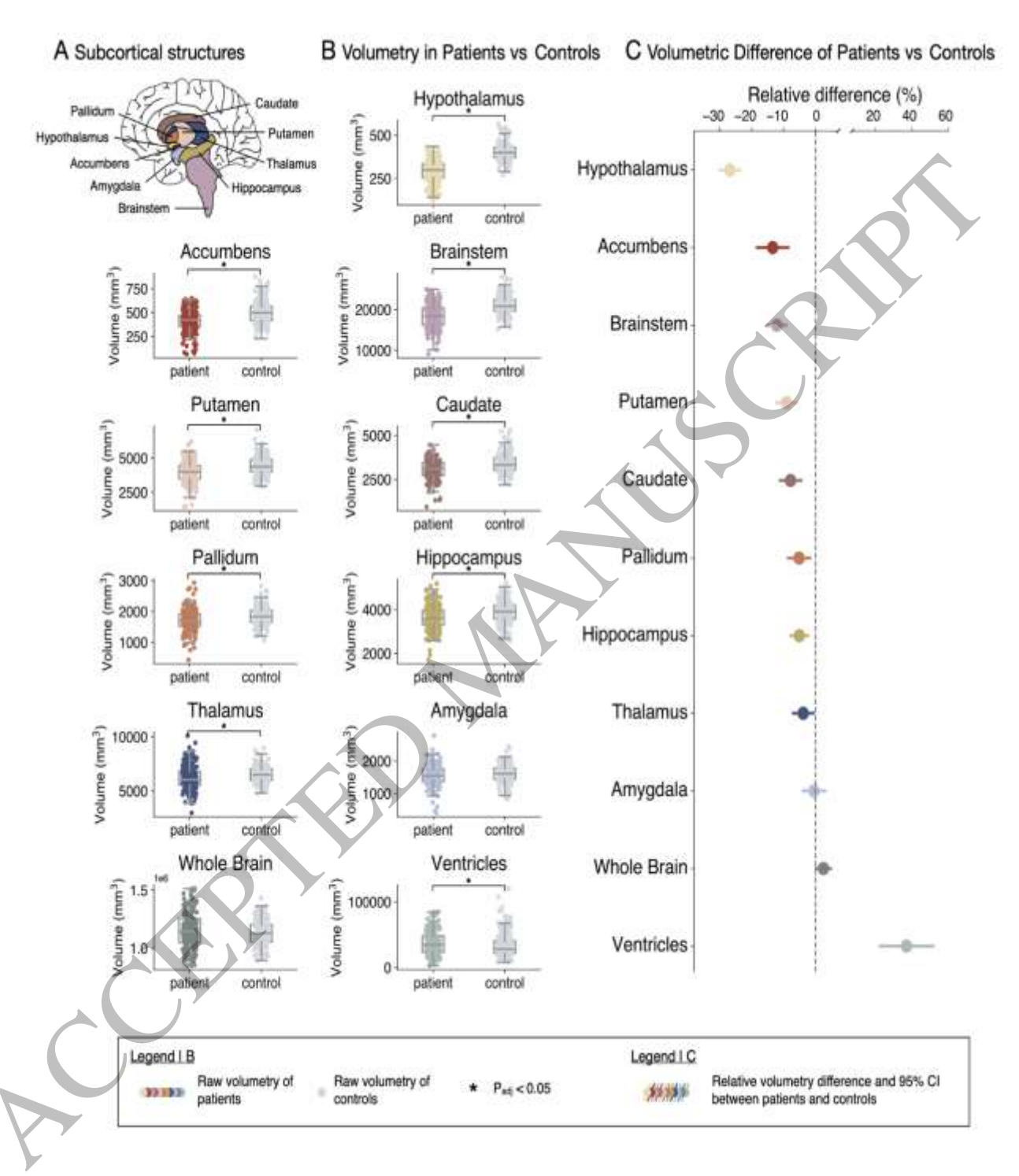
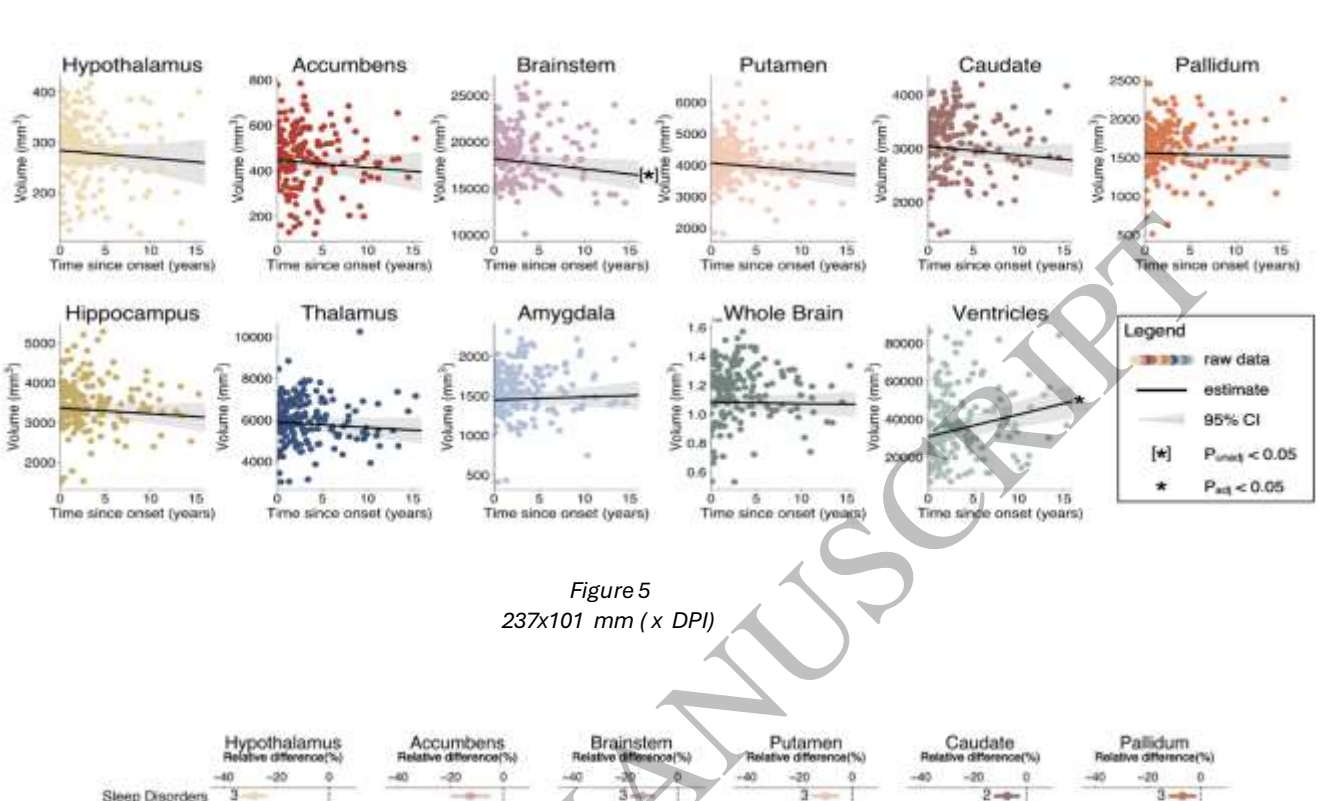
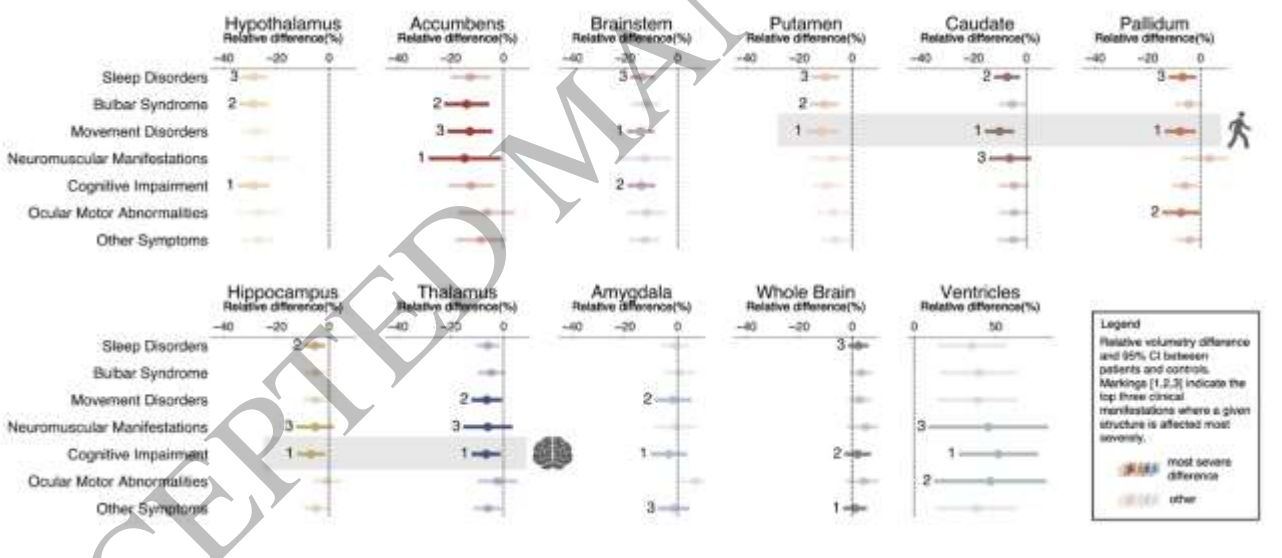


Figure 4 245x238 mm (x DPI)

2





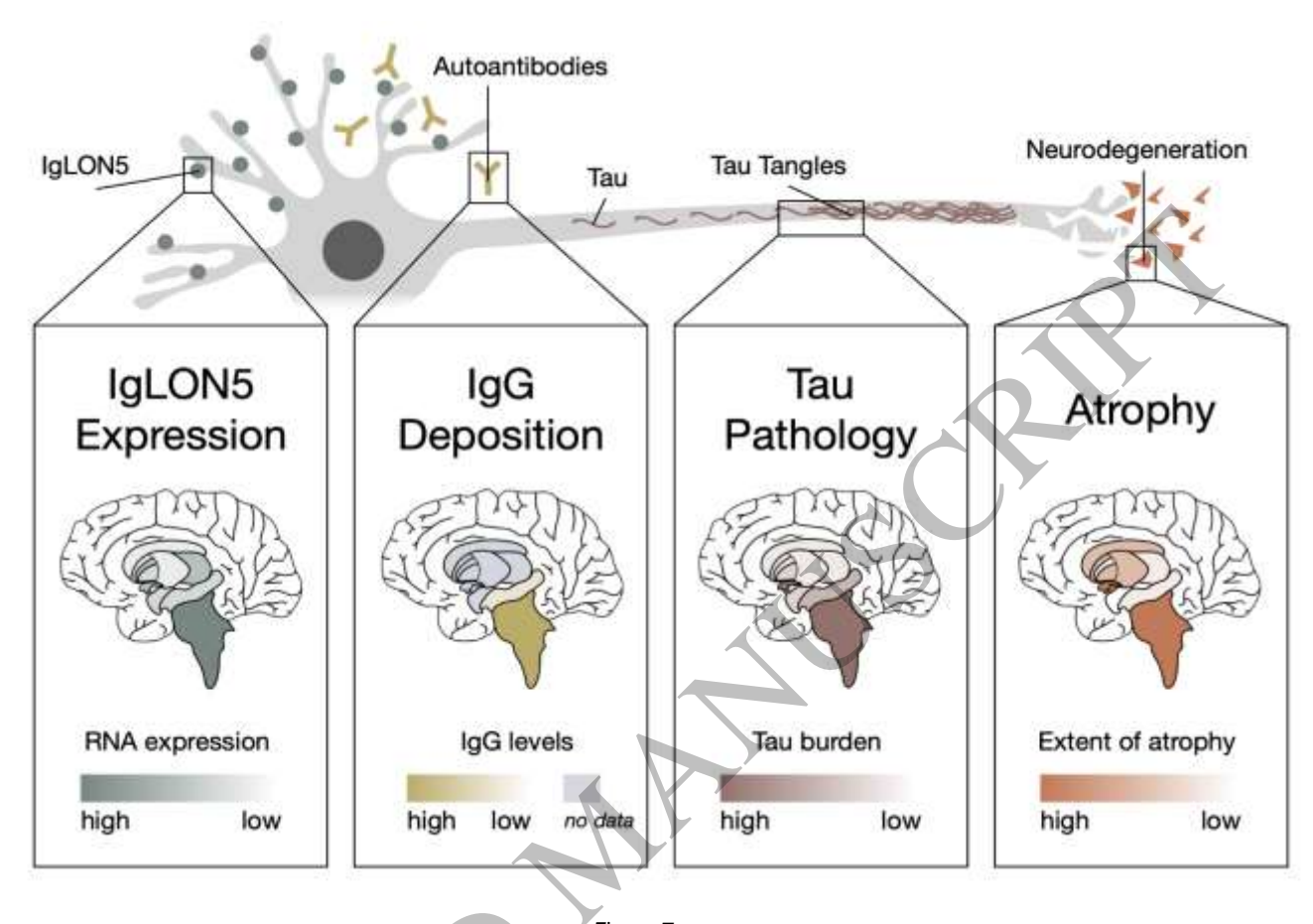


Figure 7 184x124 mm ( x DPI)